BAR Domains as Sensors of Membrane Curvature: the Amphiphysin BAR structure

Brian J. Peter, Helen M. Kent, Ian G. Mills, Yvonne Vallis, P. Jonathan G. Butler, Philip R. Evans and Harvey T. McMahon
MRC Laboratory of Molecular Biology, Hills Road, Cambridge, UK CB2 2QH

Supporting Online Material

Materials & Methods

cDNAs and Protein expression

Full-length arfaptin2 in the expression vector pGEX6P2 was a gift from Steve Gamblin (National Institute for Medical Research, London, UK), and the cDNA for *Drosophila* amphiphysin was a gift from Cahir O'Kane (Univ. of Cambridge, Cambridge, UK). cDNA for centaurinβ2 (KIAA0041) was a gift from the Kazusa DNA research institute, Chiba, Japan. cDNAs for human BRAP1/Bin2 (5722815), mouse nadrin2 (3500822) were gifts from the I.M.A.G.E. consortium. Oligophrenin1 was cloned from a rat brain library, and amphiphysin1 (residues 1-377) and 2 (residues 1-422) were cloned from a rat brain library as previously described (*S1*). Derivatives and mutants were subcloned into pGEX4T1 or 4T2, expressed in *E. coli* BL21 cells, purified by glutathione-affinity, cleaved with thrombin, and further purified by ion exchange chromatography before use. Clathrin was purified from rat brain as described on www2.mrc-lmb.cam.ac.uk/groups/hmm/techniqs/CCVprep.htm. CD spectra were measured at 20°C in 5mM HEPES, pH 7.4, 150mM NaCl using a Jobin Yvon CD6.

Protein crystallization

Drosophila amphiphysin (residues 1-245) was expressed as an NH_2-terminal GST fusion protein in minimal medium supplemented with selenomethionine. The protein was purified as above. Crystals were grown by vapour diffusion from a 2.5mg/ml protein solution in 18% PEG4000, 200mM NaCl, 1mM DTT, 20mM HEPES pH 7.4 mixed with the well solution 18% PEG 4000, 0.2M ammonium acetate, 100mM sodium citrate pH 6.0. Crystals were equilibrated in 20% glycerol for cooling to 100K. The crystal asymmetric unit contains one molecule, and the crystals belong to spacegroup $P3_121$, cell dimensions $a = b = 49.6$Å, $c = 190.3$Å, $\gamma = 120°$. A single-wavelength X-ray diffraction dataset was collected to 2.6Å resolution at the Se edge at ESRF beamline ID29 (Table S1). Images were integrated with Mosflm (*S2*) and scaled with Scala (*S3*). Two SeMet sites were located using the anomalous differences with the program Shake-and-Bake (*S4*). An additional two anomalous scattering sites at positions of the cysteine sulphur atoms were added during phasing by Sharp (*S5*). Phases were improved by solvent flattening with Solomon (*S6*). The model was built with O (*S7*) and refined with Refmac (*S8*).

Analytical ultracentrifugation

Sedimentation equilibrium experiments were performed in a Beckman Optima XL-A analytical ultracentrifuge with an An60-Ti rotor, in 10mM Tris Cl, pH 7.4, 200mM NaCl,

1mM TCEP. Sedimentation was at 11,000 rev/min, 20.0°C, with initial overspeeding at 18,000 rev/min for 6hr, to reduce the time to reach equilibrium (*S9*). Long sample columns were used, with cells loaded at a variety of initial concentrations. Scans (averaging 10 readings) were taken at 280nm at 24hr intervals, until no movement of the distribution was visible, when final scans (averaging 100 readings) were taken and assumed to be operationally at equilibrium. The rotor was then accelerated to pull the macromolecule away from the meniscus, and further scans taken to provide initial estimates of the baseline for each cell. Data were analyzed as described in detail in the supplementary information to (*S10*).

Sequence alignments

We first obtained a general BAR sequence alignment by overlaying the *Drosophila* amphiphysin and arfaptin2 BAR structures (see Figs. 1E and S5). Candidate BAR domain proteins were identified using repeated iterations of Psi-BLAST (www.ncbi.nlm.nih.gov/BLAST/) against the arfaptin and amphiphysin BAR domains. The BAR domains in these proteins were tested by aligning them with the *Drosophila* amphiphysin and arfaptin BAR domains using the clustalW function in MacVector, with an open gap penalty of 100, extend gap penalty of 0.5 and delay divergent setting of 40%. Generally when the third protein led to a correct alignment of the amphiphysin and arfaptin BARs, some charge conservation and a repeat of hydrophobic residues (green in Fig 1E) could be detected in the third BAR. Finally, candidate BARs were checked for α-helical content using Coils and Multicoil tools available at http://us.expasy.org/tools/. There should be caution in simple predictions of BAR domains given that α-helical repeats and coiled-coils are common in proteins.

Liposome sedimentation, tubulation, and lipid monolayer assays

Liposomes consisting either of 40% phosphatidylcholine, 40% phosphatidylethanolamine, 10% cholesterol, and 10% PtdIns(4,5)P_2 (Avanti Polar Lipids), total bovine brain lipids (Folch fraction 1, sigma B1502; referred to in text as brain liposomes) or total liver lipids (Avanti Polar Lipids) were resuspended at 1mg/ml in 20mM HEPES, pH 7.4, 150mM NaCl (200mM NaCl for *Drosophila* amphiphysin), 1mM DTT and sized by extrusion (*S11*). For sedimentation assays, 5μM protein was incubated with 0.6mg/ml liposomes in 100 μl of buffer for several minutes before sedimentation at 140000xg for 15 minutes in a Beckman TLA100 rotor. After spinning, supernatants were removed immediately, and pellets were resuspended in an equal volume of buffer. Proteins were subjected to SDS-PAGE, visualized by Coomassie stain, photographed with a Bio-Rad XRS system, and quantified using ImageQuant (Molecular Dynamics). For tubulation assays, proteins were incubated as above, spread on glow-discharged carbon-coated grids and negatively stained with 5% uranyl acetate. Mutations tested are described in the text, with the exception of arginines 65 and 68 in *Drosophila* amphiphysin, which were also mutated to glutamate but had no effect on binding or tubulation. Clathrin recruitment and lipid monolayer assays were performed at 20°C in 25mM HEPES pH 7.4, 125mM potassium acetate, 5mM magnesium acetate, 1mM DTT. Monolayers composed of either brain lipids or synthetic lipid mixes (which gave identical results) were formed on a 40μl buffer drop in a Teflon well. A carbon-coated

grid was placed on the droplet, proteins were injected underneath, and after 60min the grid was removed and negatively stained. A detailed protocol can be found on www2.mrc-lmb.cam.ac.uk/groups/hmm/techniqs/techniqs.htm.

Transfections and immunofluorescence

COS-7 cells were transfected with pCMV-myc vectors using GeneJuice™ (Novagen) according to the manufacturer's protocol. 28 h after transfection, cells were transferred to serum-free medium and incubated with biotinylated transferrin for 15 min before fixation with 4% PFA. Transfected cells were detected using a polyclonal anti-Myc tag antibody (Cell Signalling), biotinylated transferrin was detected with labelled avidin, amphiphysin1 and arfaptin were detected with rabbit antisera raised against purified proteins, and TGN46 was detected with an anti-TGN46 antibody (Serotech). Cells were mounted and imaged using a Radiance confocal system (Bio-Rad Laboratories). It should be noted that the amphiphysin constructs are not NH_2-terminally tagged as this prevents the tubulation in vivo (Fig. S3A), although in vitro an NH_2-terminal histidine- or glutathione-S-transferase-tag does not prevent tubulation.

Supplemental figures

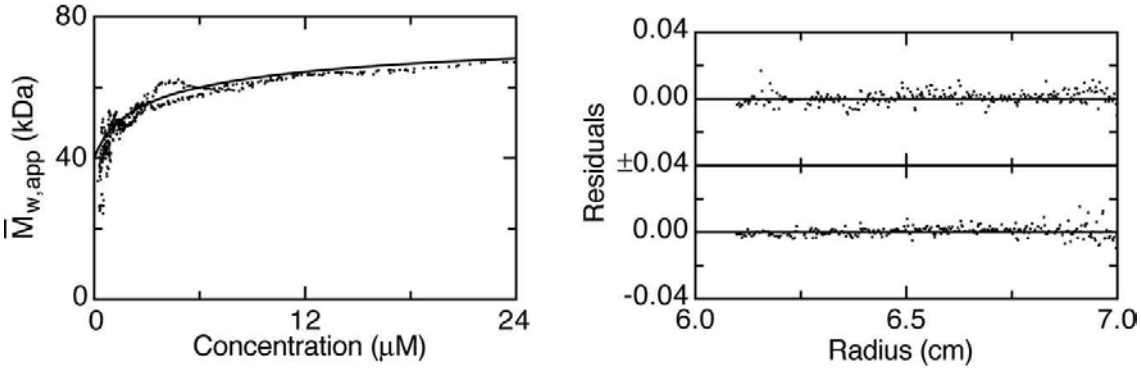

Fig. S1. Analytical ultracentrifugation of *Drosophila* amphiphysin N-BAR

The figure shows a plot of $\overline{M}_{w,app}$ against concentration (left), overlaying the individual cells, and also plots of the residuals for each cell against radius (right). In practice, the correction factor for M_1 was close to 1.0, while the concentration correction was <0.05 absorbance units. The line plotted on the $\overline{M}_{w,app}$ figure was calculated with M_1=40kDa and K_d=6μM, as derived from the fitting. The correspondence of the data with this line and, even more, the small and randomly distributed residuals for fitting the raw data, confirm that the *Drosophila* amphiphysin N-BAR reversibly dimerized under these conditions. Similar results were obtained for full-length arfaptin and centaurinβ2 BAR+PH.

A

```
dAmph----------MTENKGIMLAKSVQKHAGRAKEKILQNLGKVDR
rAmph1---------MADMKTGIFAKNVQKRLNRAQEKVLQKLGKADE
rAmph2-----MAEMGSKGVTAGKIASNVQKKLTRAQEKVLQKLGKADE
hBRAP1/Bin2-MAEGKAGGAAGLFAKQVQKKFSRAQEKVLQKLGKAVE
hBin3----MSWIPFKIGQPKKQIVPKTVERDFEREYGKLQQLEEQTRR
CeleAmph-----------MADLFNKHLKKATNRTKEKLLEGIGKAKA
ScRvs161p----------MSWEGFKKAINRAGHSVIIKN--VDK
ScRvs167p----------MSFKGFTKAVSRAPQSFRQKFKMGEQ
SPombe_Hob---------MSWKGFTKALARTPQTLRSKFNVGEI
rEndophilin1-------MSVAGLKKQFHKATQKVSEKVGGAET
mNadrin1-------------------MKKQFNRMKQLANQTVGRAEK
mNadrin2-------------------MKKQFNRMKQTVG-RAEKTEV
```

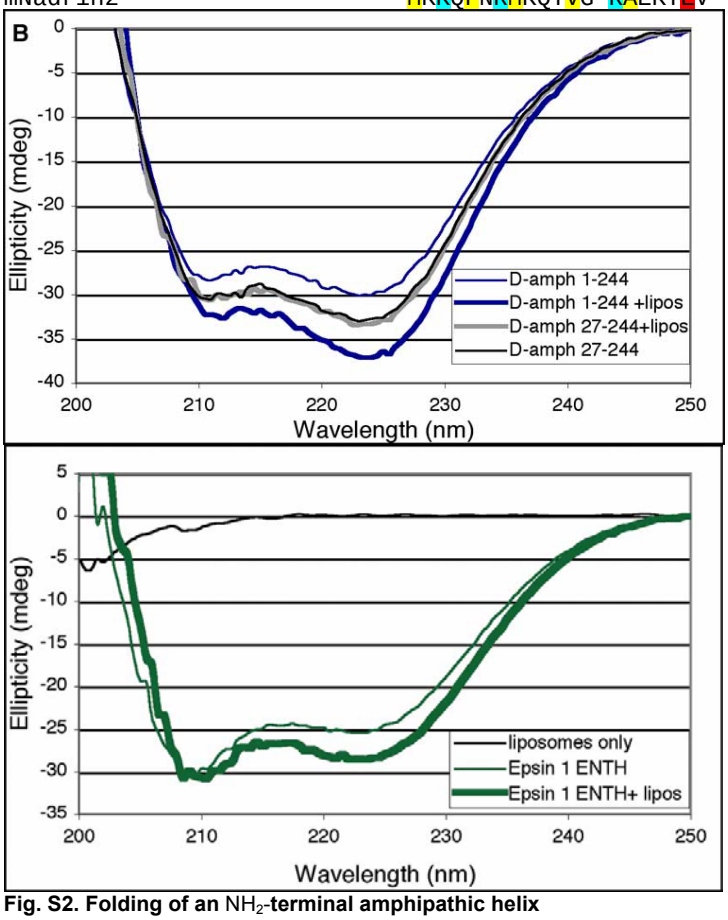

Fig. S2. Folding of an NH_2-terminal amphipathic helix

(**A**) Sequence alignment of predicted amphipathic helices in the the NH_2-termini of proteins containing an N-BAR domain. Many other BAR-containing proteins do not contain this helix and thus this may help to define BAR domain subfamilies. Hydrophobic residues are highlighted in yellow, basic residues in blue, and acidic residues in red. Rvs161p, Rvs167p and Hob are yeast homologs of amphiphysin/endophilin. Abbreviations, d, Drosophila; r, rat; h, human; Cele, C. elegans; Sc, Saccharomyces cerevisiae; Spombe, Schizosaccharomyces pombe; m, mouse. (**B**) Top, Circular dichroism (CD) spectra of the N-BAR (residues 1-244) or BAR (residues 27-244) domain of *Drosophila* amphiphysin taken in the presence or absence of brain lipid liposomes. Minima at 208 and 222 nm indicate helical content; the deepening of the second minimum is typical of an increase in α-helix content. Similar results were obtained with rat amphiphysin1. Bottom, Control CD spectra showing the spectrum of liposomes only, and the effect of liposomes on Epsin1 ENTH (Epsin NH_2-terminal homology domain), which folds an extra α-helix upon lipid binding (*S12*).

The folding of the NH_2-terminal amphipathic helix in amphiphysin could aid tubulation by direct interaction with the membrane, by protein-protein interactions between dimers, or both, but we cannot distinguish them at present. In solution, analytical ultracentrifugation showed no aggregation beyond a dimer, but higher oligomers were detected by crosslinking on liposomes (not shown). Mutation of phenylalanine 9 to glutamate in amphiphysin1 reduced but did not abolish tubulation (Fig. 2E), in contrast to the effect seen in endophilin (*S13*). Mutation of lysine 15 (in *Drosophila* amphiphysin) or lysines 15 and 16 (in mammalian amphiphysin1) to glutamates had little effect.

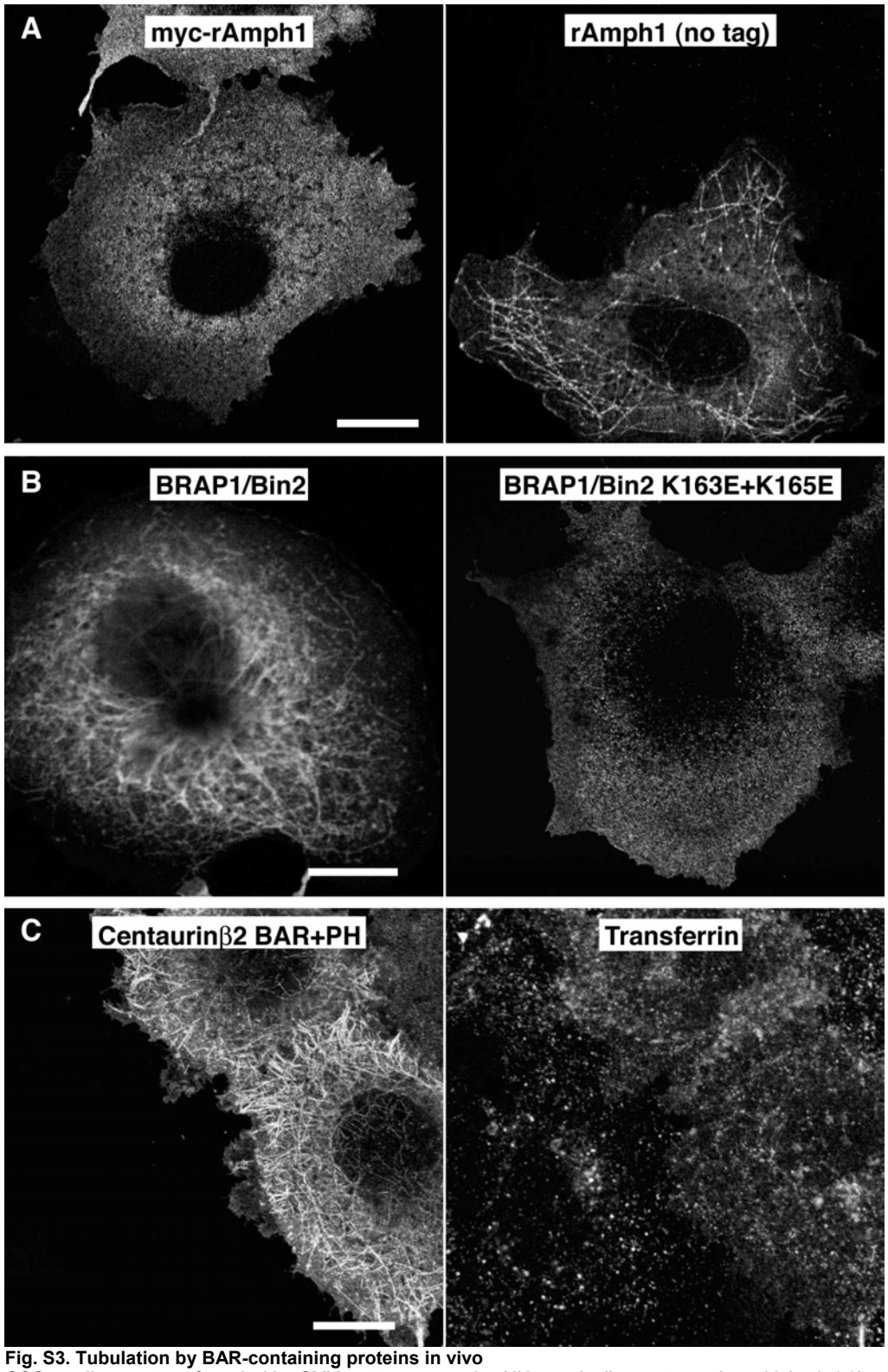

Fig. S3. Tubulation by BAR-containing proteins in vivo

COS-7 cells were transfected with pCMV vectors expressing NH_2-terminally myc-tagged amphiphysin1 (Amph1), untagged amphiphysin1, BRAP1/Bin2 N-BAR, and centaurinβ2 BAR+PH. Scale bar = 20μm. (**A**) Expression of NH_2-terminally myc-tagged amphiphysin does not cause tubulation, while expression of the untagged protein does. (**B**) Expression of the wild-

type N-BAR of BRAP1/Bin2 also causes tubulation, while the K163E+K165E mutant does not. (**C**) Overexpression of centaurinβ2 BAR+PH causes extensive tubulation and a defect in transferrin trafficking. In many cases these tubules emanated from foci within the cell but we were not able to identify the compartment. However, the PH domain of centaurinβ2 has been reported to bind PtdIns(3,5)P_2 (*S14*) a lipid implicated in endosome to multivesicular body trafficking (*S15*).

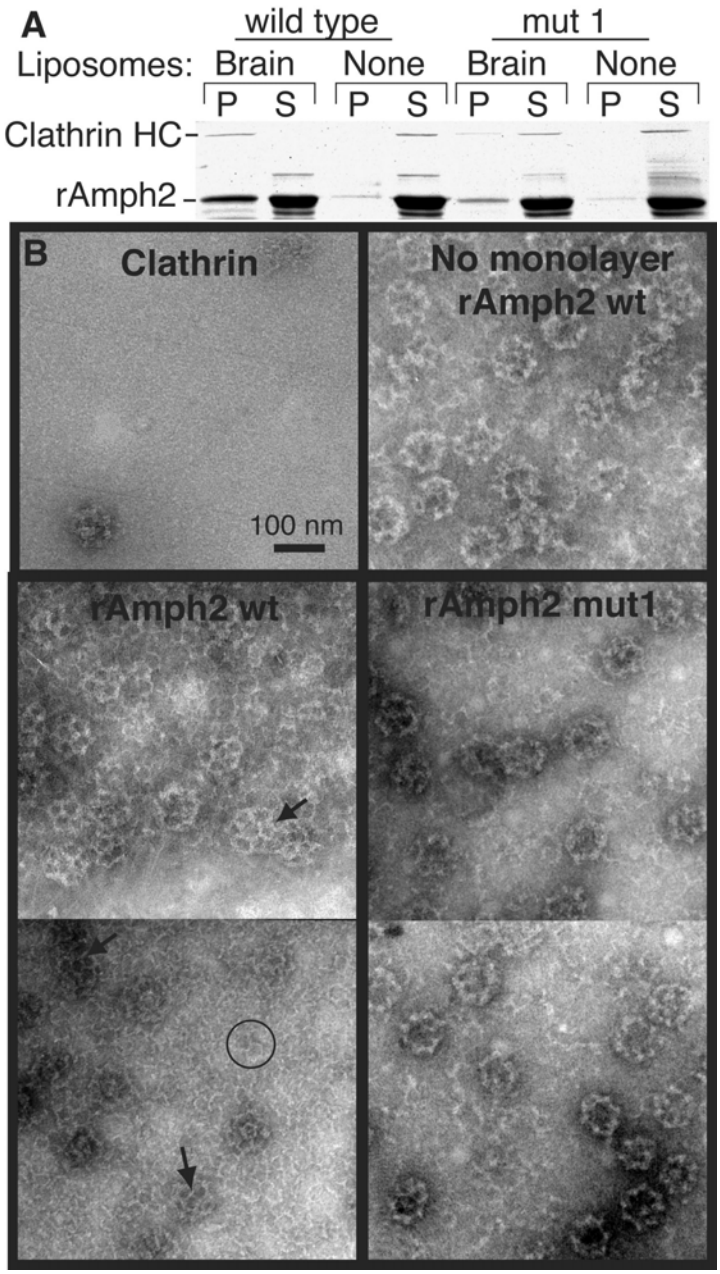

Fig. S4. Recruitment and polymerization of clathrin by amphiphysin

(**A**) Rat amphiphysin2 (rAmph2) was incubated with rat brain clathrin in the presence or absence of brain liposomes before sedimentation at 140000xg for 15min. In the Coomassie-stained gel, the first four lanes show the results obtained with wild-type protein and the last four lanes show the results obtained with the BAR mutant. Proteins in the pellet (P) or supernatant (S) were separated by SDS-PAGE. rAmph2 mut1 has the mutations K164E+K166E and was much less effective at recruiting clathrin to the membrane. Under these conditions no clathrin sedimented in the absence of other proteins. (**B**) Lipid monolayer assay demonstrating the ability of rAmph2 to recruit and polymerize clathrin. In the absence of amphiphysin, very little clathrin was on the monolayer, although occasionally a clathrin cage was seen (top left panel). When wild type rAmph2 was incubated with clathrin in the absence of lipid, the rAmph2 induced extensive polymerization of the clathrin into cages, which stuck to the grid (top right panel). However, in the presence of brain lipids, rAmph2 recruited clathrin and induced the formation of extensive lattices on the monolayers (lower left panel). The monolayers now had a high background of clathrin, and some individual clathrin triskelia were discerned (circle). Furthermore much of the clathrin was polymerized into lattice structures on the monolayer which were slightly invaginated given the presence of pentagons (arrows). In contrast the mut1 rAmph2 monolayers showed a lower background of triskelia, and now all of the polymerized clathrin was in the form of cages. Cages sitting on the surface of the monolayer can be distinguished from lattices by (a) their more defined edges, (b)

their higher electron density owing to accumulated stain inside the cage, and (c) less definition of their triskelia, together resulting in a ringlike appearance. Thus mut1 rAmph2 still polymerized clathrin in solution, which is expected as the dimerization interface and clathrin binding sites on amphiphysin were unchanged. However, mutations in the BAR seriously inhibited the ability of amphiphysin to form ordered clathrin structures on the membrane.

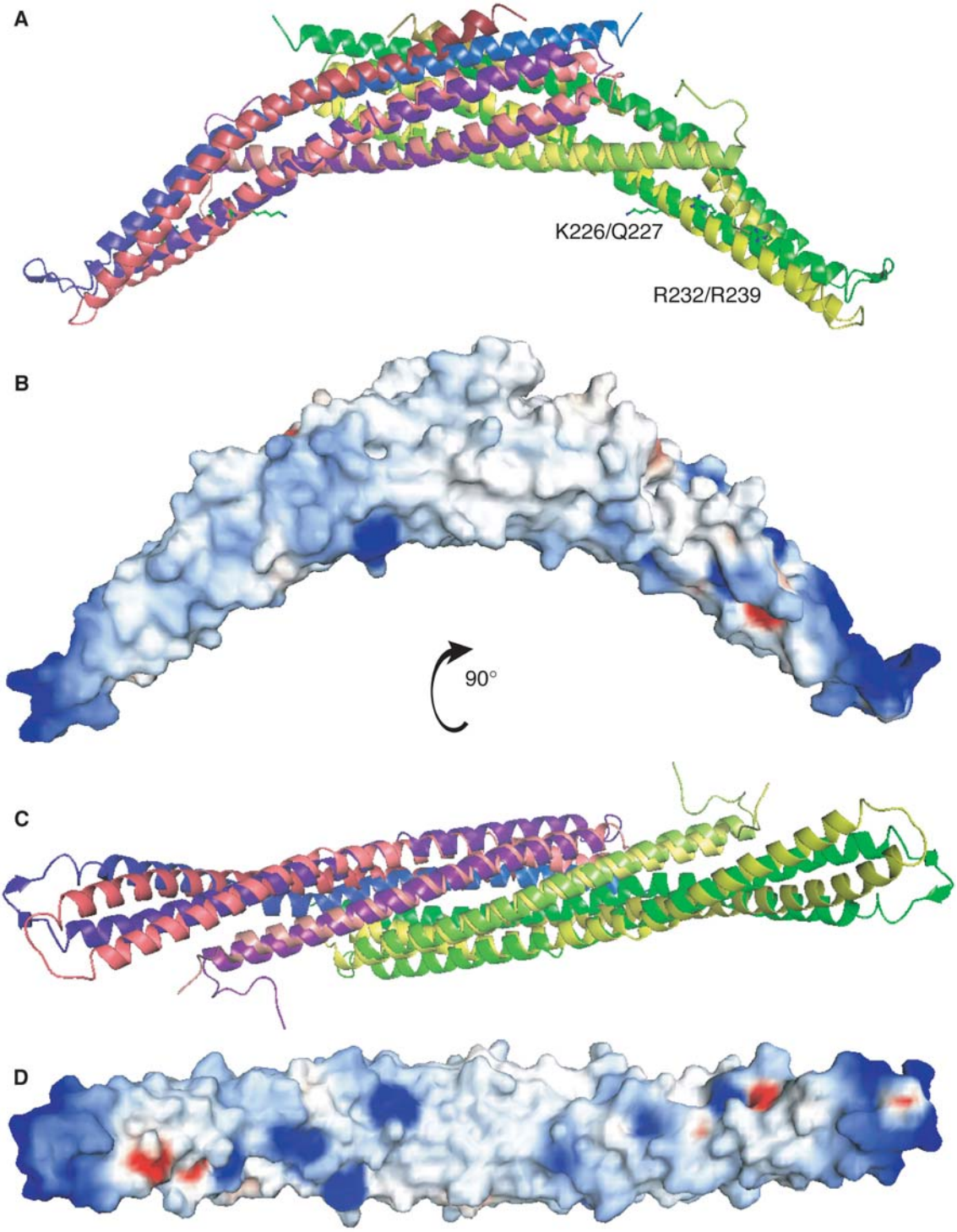

Fig. S5. Overlay of arfaptin and amphiphysin structures
(**A**) Ribbon representation of arfaptin dimer (in pink and yellow; PDB ID: 1I4D) superimposed on *Drosophila* amphiphysin (in purple and green; PDB ID: 1URU). The residues of arfaptin that were mutated are shown. (**B**) Electrostatic surface of arfaptin, as in Figure 1B,D. (**C,D**) As in (**A,B**) except the concave surface is shown.

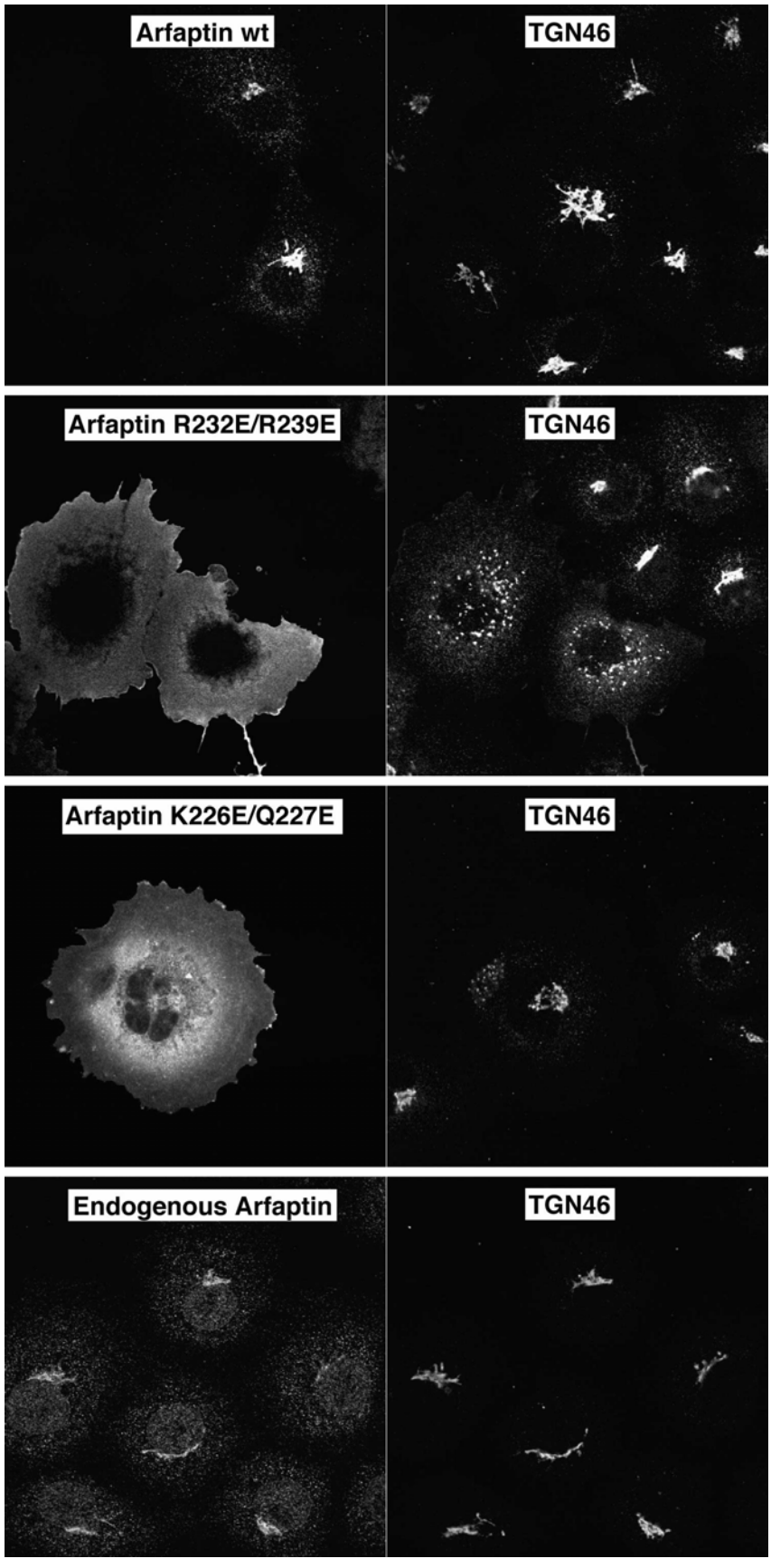
Arfaptin wt
TGN46
Arfaptin R232E/R239E
TGN46
Arfaptin K226E/Q227E
TGN46
Endogenous Arfaptin
TGN46

Fig. S6. Colocalization of wild type, mutant, and endogenous arfaptin with TGN46

Table S1. **X-ray data collection statistics**

Space Group	$P3_121$
Resolution (Å) (outer bin range)	32 - 2.6 (2.74-2.6)
Completeness	0.97 (0.86)
Multiplicity	10.2 (9.3)
Wilson plot B ($Å^2$)	65
R_{merge}*	0.134 (1.005)
R_{meas}†	0.141 (1.066)
$<<I>/<\sigma>>$	17.2(2.7)
Refinement Statistics	
R factor†† (working set)	0.230
R_{Free}	0.305
<B> ($Å^2$) (mean, overall)	57
$N_{reflections}$ (N_{free})	7786 (867)
N_{atoms} (N_{water})	1808 (37)
R_{msd} bond length (Å)	0.013

Values in parentheses apply to the highest resolution shell

* $R_{merge} = \Sigma\Sigma_i |I_h - I_{hi}| / \Sigma\Sigma_i I_h$, where I_h is the mean intensity for reflection h

† $R_{meas} = \Sigma\sqrt{(n/n-1)}\Sigma_i |I_h - I_{hi}| / \Sigma\Sigma_i I_h$, the multiplicity weighted R_{merge}

†† $R = \Sigma|F_P-F_{calc}|/\Sigma F_P$

Supplemental references and notes

S1. P. Wigge *et al.*, *Mol. Biol. Cell* **8**, 2003 (1997).
S2. A. G. W. Leslie, in *Joint CCP4 and ESF-EACMB Newsletter on Protein Crystallography No. 26*. (SERC, Daresbury Laboratory, Warrington, UK, 1992).
S3. N. Collaborative Computational Project, *Acta Crystallogr. D* **50**, 760 (1994).
S4. C. Weeks, R. Miller, *J. Appl. Cryst.* **32**, 120 (1999).
S5. E. de la Fortelle, G. Bricogne, in *Methods in Enzymology* C. W. Carter, Jr, R. M. Sweet, Eds. (1997), vol. 276, pp. 472-494.
S6. J. P. Abrahams, *Acta Cryst.* **D53**, 371 (1997).
S7. T. A. Jones, J. Y. Zou, S. W. Cowan, M. Kjeldgaard, *Acta Cryst.* **47**, 110 (1991).
S8. G. N. Murshudov, A. A. Vagin, E. J. Dodson, *Acta Cryst.* **D53**, 240 (1997).
S9. K. E. Van Holde, R. L. Baldwin, *J. Phys. Chem.* **62**, 734 (1958).
S10. I. G. Mills *et al.*, *J. Cell Biol.* **160**, 213 (2003).
S11. L. D. Mayer, M. J. Hope, P. R. Cullis, *Biochim. Biophys. Acta* **858**, 161 (1986).
S12. M. G. Ford *et al.*, *Nature* **419**, 361 (2002).
S13. K. Farsad *et al.*, *J. Cell Biol.* **155**, 193 (2001).
S14. S. Dowler *et al.*, *Biochem. J.* **351**, 19 (2000).

S15. J. D. Shaw, H. Hama, F. Sohrabi, D. B. DeWald, B. Wendland, *Traffic* **4**, 479 (2003).

Movie S1. Structure of *Drosophila* amphiphysin BAR
Ribbon representation (with a translucent electrostatic surface) of the *Drosophila* amphiphysin BAR structure rotating through a full revolution. There is a buried accessible surface area per monomer of 2380 Å, and water filled cavities are in red. Helices 2 and 3 are kinked, and the kink in helix 3 is more pronounced. These kinks could introduce limited flexibility that would influence the local curvature of the bound membrane.